Potentiation of Fcε Receptor I–activated Ca^{2+} Current (I_{CRAC}) by Cholera Toxin: Possible Mediation by ADP Ribosylation Factor

Michael A. McCloskey and Lei Zhang

Department of Zoology and Genetics, and Signal Transduction Training Group, Iowa State University, Ames, Iowa 50011-3223

Abstract. Antigen-evoked influx of extracellular Ca^{2+} into mast cells may occur via store-operated Ca^{2+} channels called calcium release–activated calcium (CRAC) channels. In mast cells of the rat basophilic leukemia cell line (RBL-2H3), cholera toxin (CT) potentiates antigen-driven uptake of $^{45}Ca^{2+}$ through cAMP-independent means. Here, we have used perforated patch clamp recording at physiological temperature to test whether cholera toxin or its substrate, Gs, directly modulates the activity of CRAC channels. Cholera toxin dramatically amplified (two- to fourfold) the Ca^{2+} release–activated Ca^{2+} current (I_{CRAC}) elicited by suboptimal concentrations of antigen, without itself inducing I_{CRAC}, and this enhancement was not mimicked by cAMP elevation. In contrast, cholera toxin did not affect the induction of I_{CRAC} by thapsigargin, an inhibitor of organelle Ca^{2+} pumps, or by intracellular dialysis with low Ca^{2+} pipette solutions. Thus, the activity of CRAC channels is not directly controlled by cholera toxin or Gsα. Nor was the potentiation of I_{CRAC} due to enhancement of phosphoinositide hydrolysis or calcium release. Because Gs and the A subunit of cholera toxin bind to ADP ribosylation factor (ARF) and could modulate its activity, we tested the sensitivity of antigen-evoked I_{CRAC} to brefeldin A, an inhibitor of ARF-dependent functions, including vesicle transport. Brefeldin A blocked the enhancement of antigen-evoked I_{CRAC} without inhibiting ADP ribosylation of Gsα, but it did not affect I_{CRAC} induced by suboptimal antigen or by thapsigargin. These data provide new evidence that CRAC channels are a major route for Fcε receptor I–triggered Ca^{2+} influx, and they suggest that ARF may modulate the induction of I_{CRAC} by antigen.

Key words: mast cells • patch clamp • Ca^{2+} imaging • Gs • brefeldin A

Introduction

Calcium influx is thought to be required for the secretion of inflammatory mediators, activation of transcription factors, and the elaboration of cytokines by rat mast cells stimulated through the high affinity receptor (FcεRI) for IgE. Cholera toxin (CT)[1] markedly potentiates FcεRI-mediated uptake of $^{45}Ca^{2+}$ (Narasimhan et al., 1988) and secretion of preformed mediators (McCloskey, 1988; Narasimhan et al., 1988) by rat basophilic leukemia cell line (RBL-2H3) mast cells. The mechanisms by which Ca^{2+} uptake and secretion are enhanced remain unknown. It is possible that the CT substrate, Gs, regulates Ca^{2+} entry by direct interaction with the presumed FcεRI-activated Ca^{2+} channel, as is thought to occur with voltage-gated Ca^{2+} channels in skeletal muscle (Hamilton et al., 1991). CT also might act indirectly by enhancing the driving force on Ca^{2+} influx via membrane hyperpolarization. Here, we test these hypotheses using perforated patch clamp recording at physiological temperature from intact RBL-2H3 cells (Zhang and McCloskey, 1995).

Experiments using radiotracer flux, Ca^{2+}-sensing fluorescent dyes, and patch clamping suggest that FcεRI-mediated Ca^{2+} influx in RBL-2H3 mast cells may occur largely by so-called store-operated or capacitative calcium entry (Ali et al., 1994; McCloskey, 1999). According to this scheme, conceived by James Putney to account for inositol trisphosphate ($InsP_3$)-induced Ca^{2+} influx in exocrine cells, depletion of lumenal Ca^{2+} from the ER activates a Ca^{2+} entry pathway in the plasma membrane (Putney, 1986, 1990). Calcium currents associated with this pathway were first observed in Jurkat human T cells and rat peritoneal mast cells, in which they are called Ca^{2+} release–acti-

Address correspondence to Michael A. McCloskey, Department of Zoology and Genetics, Iowa State University, Ames, IA 50011-3223. Tel.: (515) 294-5925. Fax: (515) 294-8457. E-mail: drmike@iastate.edu

[1]*Abbreviations used in this paper:* ARF, ADP ribosylation factor; BAPTA, 1,2-bis-(2-aminophenoxy)ethane-*N*,*N*,*N*′,*N*′-tetraacetic acid; BFA, brefeldin A; $[Ca^{2+}]_i$, concentration of ionized Ca^{2+}; CRAC, calcium release–activated calcium; CT, cholera toxin; I_{Ca}, Ca^{2+} current measured at −80 mV; I_{CRAC}, Ca^{2+} release–activated Ca^{2+} current; *I-V*, current-voltage; $InsP_3$, inositol triphosphate; InsPx, total inositol phosphates; RBL-2H3, rat basophilic leukemia cell line; Sp-cAMPS, S-p-adenosine-3′,5′-cyclic monophosphorothioate; TEA, tetraethylammonium; TNP-BSA, trinitrophenylated BSA.

vated calcium currents, or I_{CRAC} (Lewis and Cahalan, 1989; Hoth and Penner, 1992; Zweifach and Lewis, 1993). Ca^{2+} store depletion is now known to elicit Ca^{2+} influx currents superficially related to I_{CRAC} in a variety of cell types (for reviews see Fasolato et al., 1994; Berridge, 1995; Fanger et al., 1995).

The mechanism that links Ca^{2+} store depletion to Ca^{2+} influx via calcium release–activated calcium (CRAC) channels has yet to be determined, and we do not address this issue here. A separate, unanswered question is whether I_{CRAC} can be elicited or amplified through means other than Ca^{2+} store depletion. That CT enhances antigen-evoked $^{45}Ca^{2+}$ uptake into RBL-2H3 cells might suggest a role for the toxin substrate, Gs, in regulation of store-operated Ca^{2+} influx. This trimeric GTP-binding protein regulates Ca^{2+} transport in a number of different systems, through means in addition to cAMP-dependent phosphorylation. In skeletal and cardiac muscle cells, for example, direct binding of Gsα-GTP to voltage-gated Ca^{2+} channels is thought to increase the channel's open probability (Yatani et al., 1987; Hamilton et al., 1991). Several other findings point to a more general involvement of Gs in cAMP-independent regulation of Ca^{2+} and/or Mg^{2+} transport across the plasma membrane (Maguire and Erdos, 1980; Murphy and McDermott, 1992; Scamps et al., 1992; Jouneaux et al., 1993). With this precedent, it is relevant to ask whether the potentiation of antigen-evoked $^{45}Ca^{2+}$ influx by CT involves direct modulation of presumed CRAC channels by the toxin or its substrate, Gsα.

We found that CT markedly enhanced FcεRI-induced Ca^{2+} currents in RBL-2H3 cells by a mechanism that is largely independent of cAMP. CT did not affect the induction of I_{CRAC} by Ca^{2+} store depletion, per se. The enhancement of antigen-evoked I_{CRAC} was not an indirect effect of membrane hyperpolarization, nor was it a direct effect of the toxin or Gs on CRAC channel properties. Rather, CT appeared to potentiate I_{CRAC} by modulating an upstream signal other than phosphoinositide hydrolysis or Ca^{2+} release. The brefeldin A (BFA)-sensitivity of this step suggests the involvement of an ADP ribosylation factor (ARF) in the induction of I_{CRAC} via the FcεRI.

Materials and Methods

Reagents

Cholera holotoxin was from List Biological Laboratories. S-p-adenosine-3′,5′-cyclic monophosphorothioate (Sp-cAMPS) was from Biomol Research Laboratories, Inc. BFA, EGTA, dibutyryl adenosine-3′,5′-cyclic monophosphate, methylsulfoxide, nystatin, probenecid, and thapsigargin were from Sigma Chemical Co. Myo-[2^{3}H]inositol (18 Ci/mmol) was from Amersham Life Sciences. 1,2-bis-(2-aminophenoxy)ethane-*N,N,N′,N′*-tetraacetic acid (BAPTA) free acid was from Molecular Probes. BFA was used at a final concentration of 2 μg/ml, obtained by diluting 1,000-fold into growth medium a 2-mg/ml stock solution in methylsulfoxide. Thapsigargin was diluted 500-fold into external buffer (see below) from methylsulfoxide stock solutions of appropriate thapsigargin concentration. Nystatin stock solutions (50 mg/ml) in methylsulfoxide were made fresh each day. All tissue culture reagents were from GIBCO BRL. Trinitrophenylated BSA (TNP-BSA) containing ~15 mol TNP per mol BSA was synthesized as described (McCloskey, 1993).

Cell Culture

The rat basophilic leukemia (RBL-2H3) cell line (Barsumian et al., 1981) was obtained from Dr. Reuben Siraganian (National Institutes of Health, Bethesda, MD) and grown for up to 30 passages before starting fresh cultures from frozen cell suspensions. Monolayer cultures were maintained at 37°C, 5% CO_2 in MEM (Earle's salts) containing 15% heat-inactivated FBS, 100 U/ml penicillin, and 100 μg/ml streptomycin sulfate. Stock cultures were passaged by trypsinization at 4-d intervals. In two sets of experiments, Ca^{2+} currents were measured in RBL-2H3 cells obtained from the American Type Culture Collection. Ca^{2+} currents in these cells were larger than others measured in this study, whether measured at 5- or the usual 4-d postpassage. Cells harvested from stock cultures were seeded onto 12-mm round glass coverslips contained in 24-well plates (8×10^4 cells/well) and grown for 12–18 h in medium containing IgE before patch clamping. Monoclonal anti-TNP IgE, IGEL a2, (Rudolph et al., 1981) (TIB 142; American Type Culture Collection) partially purified from ascites was added to the culture medium at a protein concentration of 12 μg/ml. Just before the experiment, coverslips were rinsed in normal Ringer (see below) and placed into a recording chamber.

Electrical Recording

Except where noted otherwise, all experiments were conducted on intact cells using nystatin perforated patch recording (Horn and Marty, 1988). Methods used for conventional and perforated patch whole cell recording were as described previously (Fan and McCloskey, 1994; Zhang and McCloskey, 1995). Nystatin was used at a final concentration of 250 μg/ml, produced by a 200-fold dilution of a 50-mg/ml solution (in methylsufulfoxide) into pipette solution. All experiments were conducted at 37°C, using a Peltier device to warm the sample (Medical Systems Corp.). For most experiments, cells were voltage-clamped at a holding potential of 0 mV, and voltage ramp stimuli (−100 to +50 mV, 0.64 mV/ms) applied at 10-s intervals. A 140-ms conditioning pulse to −100 mV was applied before each ramp, in part to prevent rapid inactivation during the ramp from distorting the shape of the current-voltage (*I-V*) curve (Zhang and McCloskey, 1995). The Ca^{2+} current induced by antigen during perforated patch recording decays more rapidly than does that elicited by thapsigargin or by high concentrations of intracellular BAPTA; hereafter, I_{Ca} refers to the peak Ca^{2+} current measured at −80 mV. Micropipettes were pulled from Accu-fill 90 Micropets (B-D) and heat polished to resistances of 2–4 MΩ when filled with cesium glutamate (see below).

Conductances induced by antigen or thapsigargin were determined by computer subtraction of average traces acquired before from those taken after induction of inward Ca^{2+} currents. This method was verified on a few cells by Ca^{2+} removal, which eliminated the inward current in standard tetraethylammonium (TEA) aspartate (see below). Due to the rapidity of induction by cytoplasmic BAPTA, *I-V* plots in these experiments were determined by subtraction of traces in 0 mM extracellular Ca^{2+} from those taken in 10 mM extracellular Ca^{2+}.

The experimental averages include cells from experiments conducted on multiple days. To minimize systematic errors, on each day we assayed at least three control cells and three cells from each treatment, where up to three treatments were carried out each day. All experimental values in this paper are presented as the average ± SEM, and statistical significance was determined using the *t* test. Differences were considered significant if $P < 0.05$, and all differences listed were significant unless stated otherwise.

Solutions Used for Electrical Recording

For perforated patch recording, the pipette solution contained 55 mM KCl, 70 mM K_2SO_4, 7 mM $MgCl_2$, 5 mM glucose, and 10 mM Hepes, pH 7.35. The Cs glutamate pipette solution used for conventional whole cell recording contained 150 mM glutamic acid, 8 mM NaCl, 10 mM BAPTA $(H^+)_4$, 2.0 mM $CaCl_2$, 1.0 mM $MgCl_2$, 0.5 mM MgATP, and 10 mM Hepes titrated to pH 7.20 with CsOH; the estimated free Ca^{2+} concentration in this solution was ~30 nM. The standard bath solution was TEA aspartate, which contained 10 mM $CaCl_2$, 1 mM $MgCl_2$, 88 mM NaOH, 152.5 mM aspartic acid, 64.5 mM tetraethylammonium hydroxide, 5.6 mM glucose, and 5 mM Hepes titrated to pH 7.4 with TEA hydroxide. This composition was chosen to eliminate outward Cl^- and inward K^+ currents, and to antagonize outward K^+ currents with tetraethylammonium ion. The zero Ca^{2+} external buffer was Ca^{2+}-free TEA aspartate containing 1 mM EGTA as well as 15 mM *N*-methyl-D-glucamine aspartate in place of $CaCl_2$. The solution used for Ba^{2+} substitution contained 10 mM Ba^{2+} in place of Ca^{2+}, and 1 mM EGTA was present to chelate Ca^{2+} remaining after solution exchange.

[^{32}P]ADP Ribosylation

ADP ribosylation was carried out as described previously (McCloskey, 1988), except that reactions were terminated by addition of 1 ml ice cold 10 mM Hepes, pH 7.3, 135 mM NaCl and the membranes pelleted by centrifugation for 10 min at 20,000 *g*. Radioactive bands in the dried gels were imaged and digitized using a PhosphorImager, the image labeled in Adobe Photoshop, and printed by photomechanical transfer.

[^{3}H]inositol Phosphates Production

Antigen-stimulated production of inositol phosphates was assayed on cell monolayers as described previously (Beaven et al., 1984), with the following modifications. Cells were grown in three dram glass shell vials for 16–24 h before assay. Each vial was seeded with 2×10^5 cells in 0.5 ml medium containing 1.5 μg/ml anti-TNP IgE and 2 μCi/ml myo-[^{3}H]inositol (18 Ci/mmol). The growth medium was as described above but containing 1 rather than 15% FBS.

Calcium Imaging

Digital imaging of fura-2 loaded mast cells was carried out essentially as described for J774 monocytes (Fan and McCloskey, 1994), except that cells were imaged at 33–34°C rather than room temperature. Cells were cultured overnight under the same conditions used for setting up the patch clamp experiments, loaded with 1 μM fura-2 AM for 30 min at 37°C, rinsed, and incubated for another 30 min at 37°C before imaging in a Ca^{2+}-free external buffer containing 135 mM NaCl, 5 mM KCl, 2 mM $MgCl_2$, 5.6 mM glucose, 2.5 mM probenecid, 1 mM EGTA, and 10 mM Hepes, pH 7.4. The Ca^{2+} signal from individual RBL-2H3 cells exhibits variable lag phases after antigen addition (Millard et al., 1988). To eliminate this variability analytically, we used an Excel program which detects the first time point at which F_{340}/F_{380} crosses an arbitrarily set threshold, in this series of experiments defined as two SDs above the average resting F_{340}/F_{380} before antigen addition. These points were then aligned for each cell and the average time course of F_{340}/F_{380} calculated for the cells within the field of view.

Results

Enhancement of Antigen-induced Inward Current by CT

As observed previously (Zhang and McCloskey, 1995), addition of 50 ng/ml TNP-BSA to anti-TNP IgE-sensitized cells induced an inwardly rectifying current with a time-to-peak of 124 ± 70 s (∼131 ± 9 s in the previous study). Decrease in antigen concentration lengthened the induction, the time-to-peak being ∼200 s at 5 ng/ml and 255 s at 1 ng/ml TNP-BSA. After reaching a peak, the current normally decayed substantially within several minutes, this presumably reflecting in part the refilling of intracellular Ca^{2+} stores (Zweifach and Lewis, 1995). Fig. 1 A shows a series of *I-V* curves for the inward current induced by different concentrations of antigen. Each curve represents the average of measurements on multiple cells (see legend). Fig. 1 B gives the peak inward current measured at −80 mV as a function of antigen concentration. A graded increase in magnitude of the induced current was observed up to concentrations of TNP-BSA ∼500 ng/ml, above which the response was saturated. At 50 ng/ml, TNP-BSA induced a peak current at −80 mV of −19.1 ± 2.8 pA (n = 16), similar to the value of I_{Ca} induced by 50 ng/ml TNP-BSA in a previous study (−25.7 ± 4.7 pA) that employed the same antibody–antigen combination (IGEL a2 anti-TNP IgE and TNP_{15}-BSA).

As indicated in Fig. 1 B, pretreatment of RBL-2H3 cells with cholera holotoxin potentiated the inward current induced by subsequent exposure to antigen. In these experiments CT was applied at a concentration (2 μg/ml) and for a time (1.5–2.5 h) shown previously to maximally enhance antigen-elicited $^{45}Ca^{2+}$ uptake and secretion by RBL-2H3 cells (McCloskey, 1988; Narasimhan et al., 1988). Potentiation of the inward current was dependent upon antigen concentration, being quite strong at low antigen concentration and insignificant at an antigen concentration sufficient to saturate the induction. At a concentration of 1 ng/ml,

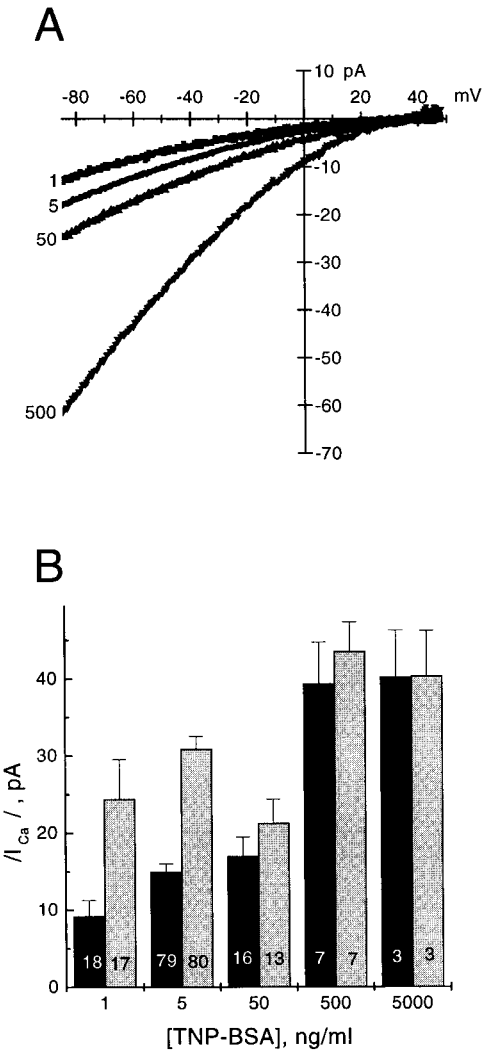

Figure 1. Effect of antigen concentration on magnitude of peak calcium current, and potentiation of Ca^{2+} current by CT. During perforated patch recording at 37°C, voltage ramps were applied from −100 to +50 mV every 5 s after the onset of induction of I_{Ca} by antigen. For each antigen concentration, the *I-V* curves recorded at the height of induction were averaged over multiple cells. (A) Average *I-V* curves obtained at four different concentrations of TNP-BSA. Numbers to left of traces indicate TNP-BSA in ng/ml. The number of cells included in average was 12, 44, 13, and 10 for concentrations of antigen of 1, 5, 50, and 500 ng/ml, respectively. For clarity, error bars not shown. (B) Plot of antigen concentration-response for induction of Ca^{2+} current. Peak current was measured at −80 mV from individual *I-V* curves obtained at different antigen concentrations. Numbers inside bars give sample size (number of cells). Black, control cells; gray, cells pretreated for 2 h with 2 μg/ml cholera holotoxin. Error bars represent SEM.

Table I. Cholera Toxin Enhances Antigen-induced I_{CRAC}

	Enhancement factor*	
TNP-BSA	Range	Mean‡
ng/ml		
1	1.9–3.8	2.8 ± 0.4 (n = 5)
5	1.2–3.3	2.2 ± 0.1 (n = 23)
50	0.6–2.6	1.5 ± 0.3 (n = 6)
500	1.1	1.1 (n = 2)

*Since I_{CRAC} varied significantly in different batches of cells, the CT enhancement of I_{CRAC} in control and CT-treated cells was compared on a day-by-day basis. Enhancement factor was calculated from results of paired experiments where antigen-induced Ca^{2+} current (at −80 mV) was measured in three to six control and three to six CT-treated cells each day.
‡Mean enhancement ± SEM of experiments conducted on n different days.

control cells exhibited an average current at −80 mV of ∼−9 pA, and CT pretreatment nearly tripled this to a value of ∼−24 pA, when all measurements are lumped in the averages. Table I summarizes the results of paired experiments conducted on different days (n = 2–23), where the enhancement each day was calculated from the average of three to six control and three to six CT-treated cells. Note that CT enhanced by nearly threefold the inward current induced by 1 ng/ml TNP-BSA, whereas the current induced by TNP-BSA at 500 ng/ml was not enhanced by CT. From these observations it appears that CT might amplify a step in the normal induction process that operates with submaximal efficiency at concentrations of TNP-BSA <500 ng/ml. Between 50 and 500 ng/ml TNP-BSA, this step has reached maximal efficiency, and potentiation by CT is not observed.

Properties of CT-enhanced Ca^{2+} Current

The ionic current elicited by antigen in CT-treated cells shared several features with that induced by antigen in control cells. For the sake of comparison, in Fig. 2 A we show average *I-V* plots obtained from 12 control and 8 CT-treated cells, each stimulated with 1 ng/ml TNP-BSA. Fig. 2 B gives average *I-V* plots obtained from 45 control and 33 CT-treated cells stimulated with 5 ng/ml TNP-BSA. The first point of similarity between the control and CT-enhanced currents is that the shape of their *I-V* curves was inwardly rectifying. In both cases the induced current had a highly positive reversal potential consistent with Ca^{2+} selectivity, and in fact Ca^{2+} is the only major permeant ion present in the TEA aspartate bath solution with such a high reversal potential. Moreover, removal of Ca^{2+} from the bath eliminated the inward current induced by antigen (data not shown). Fig. 3 A shows the result of an ion substitution experiment carried out on a CT-treated cell. Note that the antigen-induced current was carried effectively by barium ions, and that the shape of the Ba^{2+} *I-V* plot was more steeply rectifying than the Ca^{2+} *I-V* plot. This behavior was demonstrated previously for I_{CRAC} in RBL-2H3 cells, whether I_{CRAC} was elicited by antigen (Zhang and McCloskey, 1995) or induced by intracellular dialysis with a solution buffered at very low free Ca^{2+} (Hoth, 1995). Together, these observations suggest that CT amplifies the same Ca^{2+} current (I_{CRAC}) as that activated by antigen alone.

The Ca^{2+} current through CRAC channels inactivates

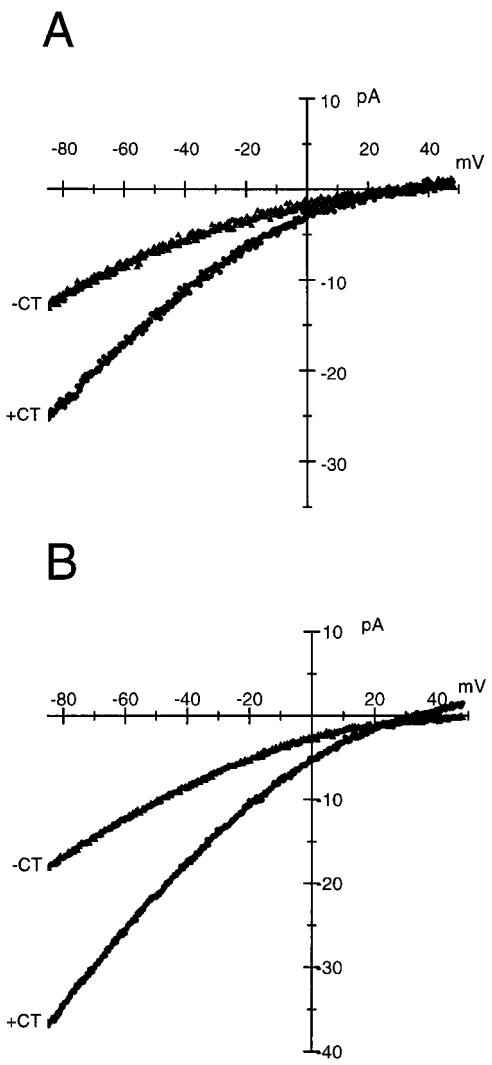

Figure 2. Average *I-V* curves for antigen-induced Ca^{2+} current in control and CT-treated cells obtained during perforated patch recording at 37°C. (A) TNP-BSA = 1 ng/ml. Average plots include 12 control and 8 CT-treated cells. (B) TNP-BSA = 5 ng/ml. n = 45 control and 33 CT-treated cells. Note similarity of *I-V* plots in control and CT-treated cells, including the highly positive reversal potential.

on two different time scales. Rapid but partial inactivation occurs after step changes of membrane potential from 0 mV to hyperpolarized voltages (Hoth and Penner, 1993; Zhang and McCloskey, 1995). Recovery from such voltage-dependent inactivation is complete within 2 s or less of returning the potential to 0 mV. Fig. 3 B shows average traces of normalized membrane current obtained from three control and three CT-pretreated cells, in each of which the Ca^{2+} current was induced by 5 ng/ml TNP-BSA. In control cells, the Ca^{2+} current inactivated by 56 ± 6% (n = 3) within 100 ms of step hyperpolarization from 0 to −100 mV. This level of steady-state inactivation is essentially equal to that reported for the Ca^{2+} current induced by 50 ng/ml TNP-BSA, i.e., a 10-fold higher level of antigen (Zhang and McCloskey, 1995). The antigen-induced current inactivated to a similar extent (62 ± 6%; n = 3) in

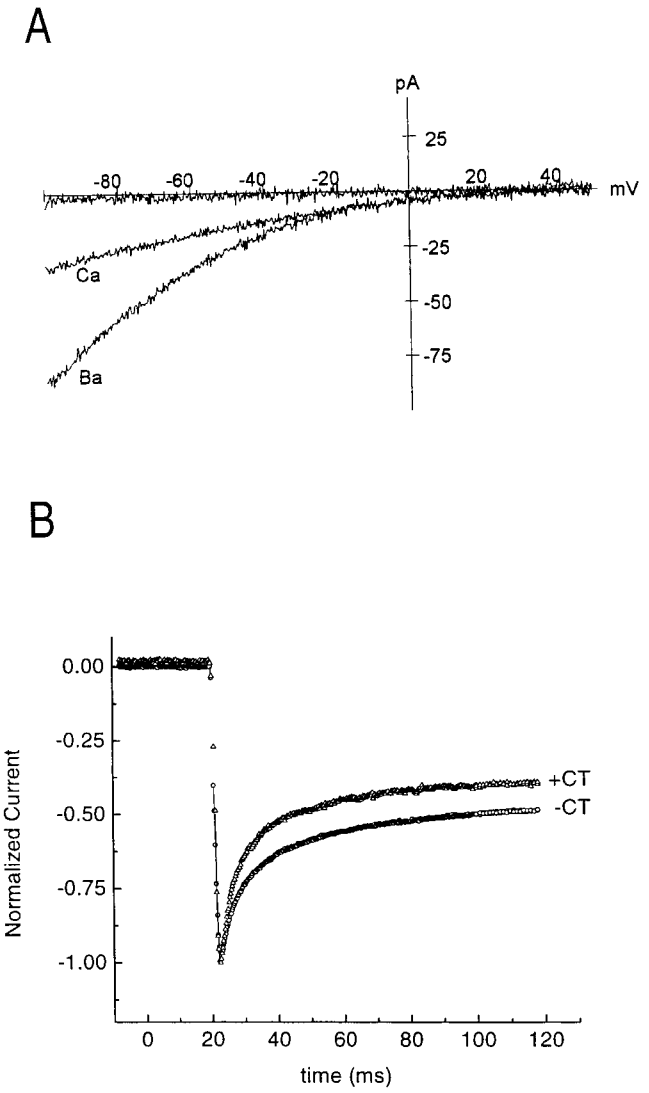

Figure 3. CT-enhanced current has *I-V* characteristics, ionic selectivity, and rapid inactivation typical of I_{CRAC}. (A) Ion substitution experiment on CT-treated cell in which inward current was evoked by TNP-BSA. Upper trace is preinduction current, and lower traces were recorded in 10 mM Ca^{2+} or 10 mM Ba^{2+} (plus 1 mM EGTA and no added Ca^{2+}). Note that Ba^{2+} permeates the CT-sensitive pathway and the Ba^{2+} current rectifies more strongly than does Ca^{2+} current, as previously shown for antigen-induced I_{CRAC} in control cells (Zhang and McCloskey, 1995). (B) Antigen-induced Ca^{2+} current undergoes rapid inactivation to similar degrees in control and CT-treated cells. After induction of Ca^{2+} current by TNP-BSA (5 ng/ml), voltage steps to −100 mV were applied from the holding potential of 0 mV. Average traces for three control and three CT-treated cells are shown. Steady-state inactivation at 100 ms was 56 ± 6% in control, and 62 ± 6% in CT-treated cells, an insignificant difference. Perforated-patch recording at 37°C for both A and B.

CT-treated cells, a further point of similarity between the control and CT-enhanced Ca^{2+} currents. Moreover, this demonstrates that the enhancement of I_{Ca} by CT was not due to reduced voltage-dependent inactivation. That is, because I_{Ca} was measured from *I-V* plots obtained by ramp stimulation after a 140-ms conditioning pulse to −100 mV, if the extent of inactivation during this prepulse was less in CT-treated than in control cells, then the value of I_{Ca} would be greater in the CT-treated than in control cells. Clearly, the potentiation of I_{Ca} by CT was not due to diminished voltage-dependent inactivation in CT-treated cells.

In principle, the magnitude of the peak Ca^{2+} current might reflect a balance between rates of activation and slow inactivation (Zweifach and Lewis, 1995). If so, CT could increase the peak I_{Ca} by enhancing the rate of activation or reducing the rate of slow inactivation. But an increased rate of activation or a decreased rate of inactivation should reduce the average time-to-peak. The average time-to-peak was about the same in control and CT-treated cells. For example, at 5 ng/ml of TNP-BSA the average time-to-peak was 205 ± 29 s (n = 27) in control and 238 ± 24 s (n = 25) in CT-treated cells, an insignificant difference. That CT did not reduce the time-to-peak suggests that alteration of activation or inactivation rates does not cause the marked enhancement of I_{Ca}.

We can also exclude the possibility that the large enhancement of Ca^{2+} influx currents by CT resulted from the induction of I_{Ca} by CT itself. As noted in Materials and Methods, the *I-V* curves shown in Figs. 2 and 3, as well as others used to derive the data shown in Fig. 1 and Table I, were obtained by computer subtraction of averaged traces taken before antigen addition. Thus, the measured currents did not contain any contribution from I_{Ca} that might have been induced by pretreatment with CT alone. It is still relevant to ask whether CT treatment, per se, induced I_{Ca}. If it did, then by the time electrical recording was begun, the magnitude of any induced Ca^{2+} current was minuscule, much smaller than the extra ~15 pA of current observed at 1 or 5 ng/ml TNP-BSA (Fig. 1 and Table I). Thus, a difference *I-V* plot of average ramp currents obtained from 35 control cells subtracted from 20 CT-treated cells—all recorded before exposure to antigen—was linear through the origin (data not shown). The slope reflects a very small increase in nonspecific leak conductance in the CT-treated cells (<1 pA at −80 mV), rather than the induction of I_{CRAC} by CT. The large enhancement of antigen-induced I_{Ca} by CT was not caused by antigen-independent induction.

Induction of I_{Ca} Is Not Enhanced by Elevation of cAMP

CT elevates cAMP levels in RBL-2H3 cells (McCloskey, 1988; Narasimhan et al., 1988), presumably through ADP ribosylation of Gs and activation of adenylyl cylcase. If the enhancement of I_{Ca} by CT is due to chronic elevation of cAMP, then cell-permeant cAMP mimetics should reproduce the effect of the toxin. To test this idea, cells were preincubated for 1.5–3 h with the cell-permeant and phosphatase-resistant cAMP analogue, Sp-cAMPS (100 μM), and then permeabilized and subjected to voltage-clamp recording in the presence of this compound. Treatment with Sp-cAMPS caused a modest but statistically insignificant increase in antigen-elicited inward Ca^{2+} current, considerably less than the enhancement caused by CT in the same experiments. The average Ca^{2+} current elicited by 5 ng/ml TNP-BSA was −14.0 ± 1.6 pA in control cells (n = 18), and −19.9 ± 2.5 pA in cells treated with Sp-cAMPS (n =

18). In these experiments, CT potentiated antigen-induced I_{Ca} by 2.3-fold. We also tested the effect of another cell-permeant analogue of cAMP, dibutyryl cAMP, which at a concentration of 0.5 mM causes modest potentiation of antigen-induced secretion in RBL-2H3 cells (McCloskey, 1988). Dibutyryl cAMP at this concentration had no statistically significant effect on antigen-induced I_{Ca}. Thus, chronic elevation of cAMP does not mimic the enhancement of I_{Ca} by CT. Although it is conceivable that CT could amplify a cAMP transient induced by antigen binding, and in this way affect I_{Ca}, previous studies have shown that cross-linkage of the FcεRI does not elevate cAMP in RBL-2H3 cells (Morita and Siraganian, 1981), and pretreatment with CT does not unmask a latent rise in cAMP (McCloskey, 1988). Thus, although elevation of cAMP may contribute, it is not the major factor in the large enhancement of antigen-elicted I_{Ca} by CT.

CT Does Not Potentiate I_{Ca} Induced by Thapsigargin or BAPTA

The macroscopic Ca^{2+} current, I_{Ca}, is directly proportional to the number of Ca^{2+} channels in the plasma membrane, their unitary conductance, and their probability of being open. Previous findings suggest that in RBL-2H3 cells, the Ca^{2+} currents associated with both antigen- and thapsigargin-induced Ca^{2+} influx (Ali et al., 1994) are carried by the same Ca^{2+} channel (Zhang and McCloskey, 1995). Thus, if CT were to increase the open probability or unitary conductance of this species, it should potentiate the macroscopic Ca^{2+} current induced by suboptimal concentrations of thapsigargin, as it does for the antigen-induced current. As demonstrated in Fig. 4, thapsigargin at 50 pM induced I_{CRAC} equivalent to that induced by suboptimal antigen (1 ng/ml TNP-BSA). Whereas CT enhanced the antigen-induced current by ~2.2-fold at 1 ng/ml TNP-BSA, it did not affect the current induced by 50 pM thapsigargin. Indeed, CT did not significantly affect the Ca^{2+} currents induced by thapsigargin at any concentration tested. This suggests that neither CT nor its substrate Gs, modifies the unitary conductance or open probability of CRAC channels in RBL-2H3 cells.

Thapsigargin presumably activates I_{CRAC} by inhibiting the Ca^{2+} pumps of the ER (Thastrup et al., 1990) and allowing passive leak of stored Ca^{2+} into the cytosol. In mast cells, I_{CRAC} can also be induced by dialysis of the cell cytoplasm with low Ca^{2+} pipette solutions buffered with high concentrations of the calcium chelator BAPTA (Fasolato et al., 1993), conditions which prevent re-uptake of Ca^{2+} by the ER. We tested the effect of CT on I_{CRAC} induced by dialysis with BAPTA. Cells were preincubated with 2 μg/ml CT for 1.5–3 h, then standard whole cell recording was performed at 37°C with a Cs glutamate pipette solution containing 10 mM BAPTA (~30 nM free Ca^{2+}). CT failed to enhance the Ca^{2+} current induced by dialysis with BAPTA, just as it had failed to enhance the thapsigargin-induced current. The peak current at −80 mV was −30 ± 6 pA in control cells (n = 10) and −28 ± 5 pA in cells pretreated with CT (n = 10). These data provide further evidence that neither CT nor Gs acts directly on the CRAC channels, and they point to the intervention of CT at a step upstream of the channel itself.

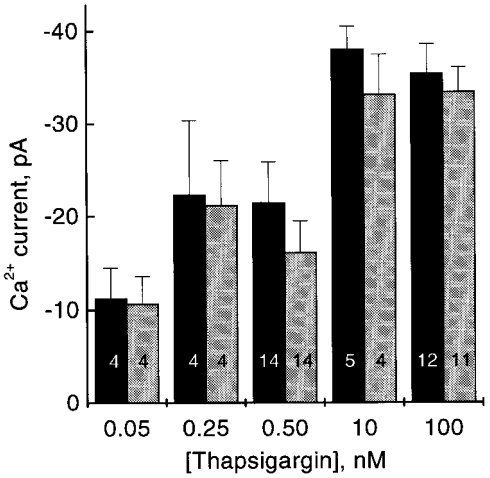

Figure 4. Dose-response plot for induction of I_{CRAC} by thapsigargin during perforated patch recording at 37°C. Black bars are control cells and gray bars CT-treated cells. Note that pretreatment with CT did not amplify the Ca^{2+} current induced by thapsigargin at any concentration. This indicates that the open probability of CRAC channels is not modulated by direct binding to Gs or toxin molecules. Numbers inside of bars give sample size. Error bars represent SEM.

Phosphoinositide Hydrolysis and Calcium Release

Because the CT target lies upstream of the Ca^{2+} channels, a logical candidate is the Ca^{2+}-releasing messenger, $InsP_3$. Augmentation of $InsP_3$ formation should enhance I_{CRAC} at low antigen levels, but as antigen concentration is increased, a point should be reached at which sufficient $InsP_3$ is generated to completely release the Ca^{2+} stores. No further effect of CT on I_{CRAC} induction is expected beyond this concentration of antigen. In principle, this mechanism could explain why CT selectively amplifies antigen- but not thapsigargin-induced I_{CRAC}, because thapsigargin releases stored Ca^{2+} independent of phosphoinositide hydrolysis. To test this hypothesis we measured antigen-stimulated production of [^{3}H]inositol phosphates (InsPx) in control cells and cells pretreated for 2 h with 2 μg/ml CT. InsPx were measured at 200 s after antigen addition, a time which corresponds to the peak Ca^{2+} current induced by 5 ng/ml TNP-BSA. As indicated in Fig. 5, at a concentration of TNP-BSA (5 ng/ml) for which CT amplified the induced current by 220%, CT did not significantly affect hydrolysis of [^{3}H]labeled inositol phospholipids. For longer preincubations (5–6 h), CT caused a modest enhancement of antigen-stimulated InsPx production (McCloskey, 1988). Thus, it appears that CT does not potentiate I_{CRAC} via enhancement of phosphoinositide hydrolysis.

To further test the hypothesis that CT potentiates I_{CRAC} by accentuating antigen-induced Ca^{2+} release, we measured cytosolic free calcium after stimulation of IgE-sensitized RBL-2H3 cells with antigen. Cells were pretreated or not with 2 $\mu g/ml^{-1}$ CT for 1 h, loaded with 2 μM fura-2 AM for 30 min, kept for another 30 min at 37°C, and then stimulated with 5 ng/ml^{-1} TNP-BSA on the stage of the microscope. Cells were plated at the same low density as during patch clamping, which limited the average number

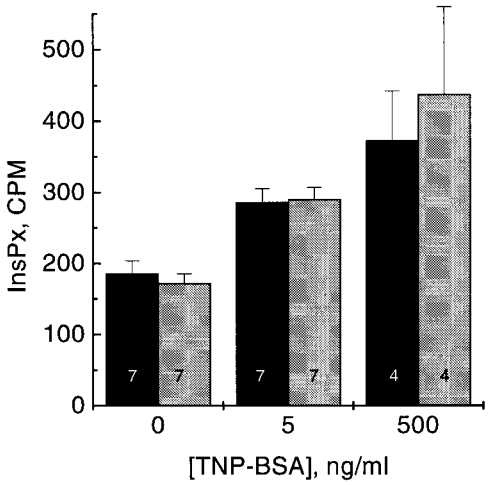

Figure 5. Antigen-stimulated release of total inositol phosphates (InsPx) in control and CT-pretreated cells. Cell monolayers were preincubated for 2 h with MEM ± 2 μg/ml CT, rinsed, and stimulated for 200 s with TNP-BSA at the indicated concentration. Black, control cells; gray, CT-pretreated cells. CT did not significantly affect InsPx production under conditions where antigen-induced I_{CRAC} was amplified 2.2-fold. For much longer preincubations, modest enhancement was observed. Error bars give SEM of four to seven experiments, each run in triplicate.

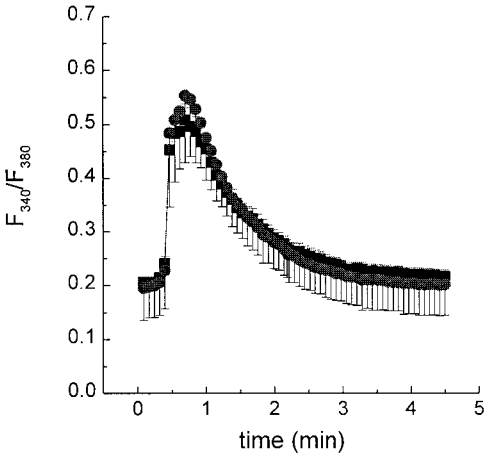

Figure 6. CT does not enhance the rate or extent of antigen-induced Ca^{2+} release in RBL-2H3 cells. Fluorescence from fura-2 loaded cells was digitally imaged and the fluorescence ratio (F_{340}/F_{380}) plotted at 4-s intervals. A thresholding routine was used to align the $[Ca^{2+}]_i$ peaks from cells on each coverslip. Averages for nine control (filled circles) and nine CT-treated coverslips (filled squares) are shown, representing a total 150 cells for each treatment. Error bars represent SEM and face downward for CT-treated cells and upward for control cells.

per field to ~17. Nine control and nine CT-treated monolayers were examined over a 5-min period, during which 90.2 ± 4.8% of the control and 91.6 ± 3.6% of the CT-treated cells responded to antigen. Resting calcium levels were the same in the two populations, the fluorescence ratio F_{340}/F_{380} being 0.18 ± 0.02 in control and 0.19 ± 0.01 in CT-treated cells. The average lag between antigen addition and the initial rise in $[Ca^{2+}]_i$ was the same in control (1.92 ± 0.25 min) and CT-treated cells (1.80 ± 0.11 min), as was the maximum rate of rise of $[Ca^{2+}]_i$ (2.28 ± 0.15 min^{-1} in control vs. 2.19 ± 0.11 min^{-1} in CT-treated cells). Variability of lag phases was removed by thresholding, and the initial $[Ca^{2+}]_i$ peaks were aligned as described in Materials and Methods. The corresponding plots as shown in Fig. 6 show no statistically significant difference between the peak heights or the rate of decline in $[Ca^{2+}]_i$ in control and CT-treated cells. By these criteria, it does not appear that the ability of CT to double antigen-evoked I_{CRAC} is due to enhanced Ca^{2+} release from internal compartments.

Effects of BFA on Ca^{2+} Current

In addition to their cell surface localization, some heterotrimeric G proteins, including Gs, are located on intracellular membranes, where they regulate vesicle trafficking (Helms, 1995). CT enhances transcytosis of vesicles containing the poly Ig receptor as well as the apical transport of influenza hemagglutinin (Bomsel and Mostov, 1993; Pimplikar and Simons, 1993). Conceivably, CT affects the trafficking of vesicles, including those bearing CRAC channels, to or from the plasma membrane of RBL-2H3 cells. To test this hypothesis, we examined the effects of BFA on CT-enhanced I_{Ca}. BFA is a fungal metabolite that inhibits certain vesicle transport and fusion steps by inhibiting GTP/guanosine diphosphate exchange on ARF proteins, thereby blocking their association with membranes (Klausner et al., 1992; Randazzo et al., 1993). Cells were preincubated with BFA, CT, or BFA plus CT for 1.5–3 h, and voltage-clamp measurements performed after patch permeabilization. BFA was present throughout the nystatin permeabilization and recording periods. At a concentration (2 μg/ml) that had no significant effect on I_{Ca} induced by suboptimal antigen (5 ng/ml TNP-BSA), BFA reduced by 84% the enhancement of I_{Ca} by CT (Fig. 7). This implicates the involvement of ARF in the enhancement of I_{CRAC} by CT.

We next determined whether BFA reduced the enhancement of I_{Ca} through blocking the ADP ribosylation of Gsα, rather than by modulating a function of Gs so modified. This is an important question because BFA prevents the membrane association of ARF proteins, which can enhance ADP ribosylation of Gsα in vitro (Kahn and Gilman, 1986). We examined the effect of BFA on ADP ribosylation of endogenous Gsα by assaying the CT-mediated [^{32}P]ADP ribosylation of Gs in membrane preparations. Cells were pretreated with 2 μg/ml CT in the presence or the absence of 2 μg/ml BFA. Membranes from control and CT-treated cells were then isolated and treated with activated CT and ^{32}P-NAD. Fig. 8 shows that pretreatment of cells with CT (Fig. 8, lane D) prevented the subsequent transfer of [^{32}P]ADP ribosyl moieties to Gsα, presumably because the acceptor arginine residue in Gsα was already substituted with nonradioactive ADP ribose from endogenous NAD. If BFA were to prevent this reaction in intact cells, then incubation of cells with both CT and BFA before membrane isolation should cause the reappearance of a radioactive band in the gel after in vitro treatment with radioactive NAD and activated CT. However, as shown in Fig. 8, lanes C and E, the presence of

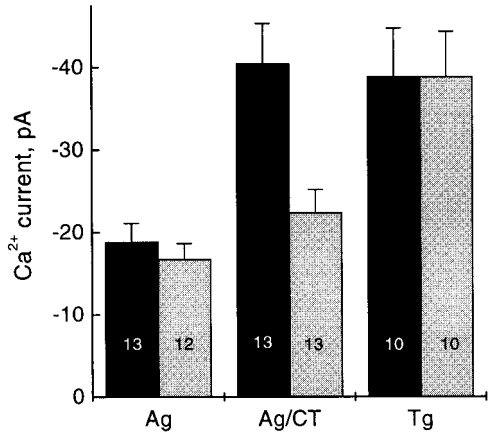

Figure 7. BFA inhibits the enhancement of antigen-induced I_{Ca} by CT. Simultaneous treatment with 2 μg/ml BFA and 2 μg/ml CT blocks by 84% the enhancement of antigen-elicited I_{Ca} by CT, whereas magnitude of Ca^{2+} current induced by suboptimal antigen alone or by optimal thapsigargin was not affected. Currents were measured using perforated patch recording at 37°C, using a TNP-BSA concentration of 5 ng/ml and a thapsigargin concentration of 100 nM. Black bars, control cells; gray bars, cells treated with BFA. Numbers inside bars give sample size.

BFA at 2 μg/ml did not interfere with ADP ribosylation either in vitro (Fig. 8, lane C) or in intact cells (Fig. 8, lane E). Thus, the inhibition by BFA of CT-enhanced I_{CRAC} is not an artifact of reduced ADP ribosylation of the CT substrate, Gs.

Could the differential effect of CT at low vs. high antigen levels indicate a progressively greater contribution of an ARF-mediated event with increase in antigen concentration? At a concentration of TNP-BSA (500 ng/ml) that induced the maximal Ca^{2+} current, BFA substantially inhibited the induction. In these experiments cells were pre-

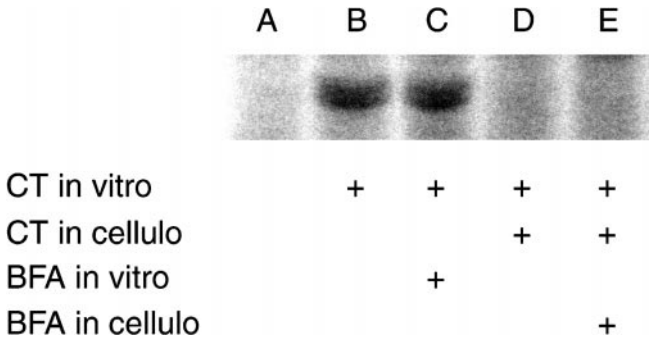

Figure 8. BFA does not inhibit ADP ribosylation of endogenous Gsα subunits by CT. Membranes were isolated from RBL-2H3 cells pretreated or not with 2 μg/ml CT with or without 2 μg/ml BFA, and then subjected to in vitro ADP ribosylation with activated CT and ^{32}P-NAD. The presumed Gsα subunits span the range of M_r from 48.9–53.2 kD. (Lane A) no CT in vitro; (lane B) control membranes; (lane C) control membranes plus 2 μg/ml BFA in vitro; (lane D) membranes from cells pretreated with CT; and (lane E) membranes from cells pretreated with CT and BFA, and subjected to [^{32}P]ADP ribosylation in vitro in the absence of BFA. Similar results were obtained in three separate experiments.

incubated with 2 μg/ml BFA for 1 h at 37°C before patch clamping, and they were also exposed to the drug during the permeabilization and induction periods. In measurements performed on 5-d cultures, the magnitude of I_{Ca} was -61.7 ± 6.6 pA ($n = 12$), whereas in BFA-treated cells, the peak I_{Ca} was -45.6 ± 4.9 pA ($n = 14$). In 4-d cultures, 500 ng/ml TNP-BSA induced I_{Ca} of -46.8 ± 2.2 pA ($n = 5$) in control, and -35.8 ± 4.3 pA ($n = 5$) in BFA-treated cells. Thus, BFA inhibited the induction of CRAC currents ~30% for both 4- and 5-d cultures, although at this sample size the difference is barely significant at $P = 0.05$.

In contrast, BFA did not affect I_{Ca} induced by thapsigargin. The average current induced by 100 nM thapsigargin was -38.9 ± 5.9 pA ($n = 10$) in control cells, and -38.9 ± 5.5 pA ($n = 10$) in cells pretreated for 1.5–2.5 h with 2 μg/ml BFA. These findings suggest that the FcεRI activates I_{CRAC} through means in addition to Ca^{2+} store depletion, and that BFA and CT affect a step unique to the antigen-induced pathway to I_{CRAC}. But if so, why were the maximal Ca^{2+} currents induced by thapsigargin and antigen similar? One clue comes from preliminary experiments on the effect of thapsigargin added after maximal induction of I_{CRAC} by antigen. Thapsigargin induced a Ca^{2+} current of -46 ± 3 pA ($n = 6$) in cells stimulated previously with optimal antigen (500 or 5000 ng/ml TNP-BSA), a 44% increase over the initial antigen-induced current in the same cells, and 21% greater than the thapsigargin-induced current in antigen-naive cells. Thus, the antigen-stimulated cells might contain a greater number of CRAC channels with a lower open probability than those in thapsigargin-stimulated cells. The latter would not be surprising, given that I_{CRAC} in RBL-2H3 cells is desensitized by protein kinase C–dependent phosphorylation (Penner et al., 1986), and this enzyme could be more active in antigen- than thapsigargin-treated cells. Moreover, thapsigargin irreversibly depletes the Ca^{2+} stores, whereas antigen causes an oscillatory Ca^{2+} signal that requires $InsP_3$, to which the $InsP_3$ receptor becomes desensitized.

Discussion

Other than a role for Ca^{2+} store depletion, the molecular mechanisms that regulate antigen-stimulated Ca^{2+} influx into mast cells are not well-understood. The observation that CT dramatically enhances $^{45}Ca^{2+}$ influx into RBL-2H3 cells suggests that this reagent might be a useful tool to study the Ca^{2+} entry pathway (Narasimhan et al., 1988). That CT amplifies both antigen-evoked I_{CRAC} and $^{45}Ca^{2+}$ influx to a similar extent bolsters the idea that CRAC channels are a major pathway for FcεRI-mediated Ca^{2+} uptake into RBL-2H3 mast cells (Zhang and McCloskey, 1995).

Two hypotheses to explain the effect of CT on $^{45}Ca^{2+}$ influx are immediately testable by patch clamping. First, it is possible that CT activates Cl^- or K^+ channels, and thereby increases the electrical force propelling Ca^{2+} entry. This indirect mechanism cannot explain the enhancement of Ca^{2+} influx currents that we observed, because voltage-clamp measurements eliminate any difference in membrane potential between control and CT-treated cells. Second, Gs might bind directly to CRAC channels and increase their open probability, as occurs with voltage-

dependent Ca^{2+} channels (Hamilton et al., 1991). This mechanism is no longer tenable, as CT did not affect the CRAC currents elicited by BAPTA or thapsigargin (at concentrations inducing submaximal or maximal I_{Ca}). Although the negative result with BAPTA could be due to loss of critical cytosolic factors during conventional whole cell recording, this is not true for the induction by thapsigargin during perforated-patch recording, nor can reduced rates of fast or slow inactivation explain the amplified I_{CRAC}.

CT by itself does not provide all signals required to activate I_{CRAC}. Rather, it appears to amplify a signal unique to the FcεRI-initiated pathway for induction of I_{CRAC}, somewhere upstream of the channels themselves. An obvious candidate for the site of intervention is the formation of Ca^{2+}-releasing second messengers. As shown in Fig. 5, at a concentration of antigen at which CT enhanced I_{CRAC} by 2.2-fold, CT did not affect antigen-stimulated phosphoinositide hydrolysis. As observed previously, prolonged incubation (6 h) with CT significantly enhanced inositol phosphates production, but this preincubation was much longer than that required for I_{CRAC} enhancement (McCloskey, 1988). In addition, others have reported that CT does not affect the FcεRI-linked production of inositol-1,4,5-trisphosphate per se (Narasimhan et al., 1988). In any case, we found that neither the rate of Ca^{2+} release nor the peak Ca^{2+} rise was greater in CT-treated than control cells, suggesting that the ability of CT to double antigen-induced I_{CRAC} is not due to enhanced Ca^{2+} release.

ARF is a monomeric GTPase that interacts with the CT-A subunit to enhance ADP ribosylation of Gsα (Kahn and Gilman, 1986). Six members of the ARF family are currently recognized, each of which reversibly associates with membranous organelles (Hosaka et al., 1996). In their GTP-bound state, ARF proteins activate phospholipase D (Brown et al., 1993; Cockcroft et al., 1994) and promote the assembly of protein coats that mediate vesicle budding and transport (for reviews see Donaldson and Klausner, 1994; Boman and Kahn, 1995; Moss and Vaughn, 1998). ARF binds to both Gs and CT-A in vitro (Boman and Kahn, 1995; Colombo et al., 1995), and it is possible that either interaction might perturb ARF function in cellulo. Together with ARF, Gs is present on the TGN, where it regulates vesicle budding (for review see Helms, 1995). These observations suggest that CT might enhance I_{CRAC} by modulating ARF activity. We tested this idea with BFA, a fungal metabolite that prevents membrane association of ARF and inhibits ARF-dependent functions (Klausner et al., 1992). That BFA strongly inhibited the enhancement of I_{CRAC} by CT, and in preliminary experiments partially inhibited the induction of I_{CRAC} by optimal antigen, suggests that ARF proteins may participate in the induction of I_{CRAC} by antigen.

Further studies are necessary to confirm this idea, but it is tempting to speculate that the FcεRI, through means in addition to Ca^{2+} store depletion, somehow modulates an ARF function that controls CRAC channel activity. Interestingly, cross-linkage of the FcεRI in RBL-2H3 cells inhibits redistribution of ARF and β-COP from Golgi membranes to the cytosol after cell permeabilization (De Matteis et al., 1993). Cross-linkage of FcεRI also increases the rate of vesicular transport of ^{35}S-labeled proteoglycans from distal Golgi compartments to the plasma membrane, a putative ARF-dependent process (Buccione et al., 1996).

If CT amplifies a signal linking the FcεRI to ARF, how could this enhance I_{CRAC}? One possibility stems from the observation that pretreatment of PC12 cells with CT enhances the cell-free formation of both constitutive secretory vesicles and immature secretory granules from the TGN (Leyte et al., 1992). In MDCK epithelial cells, CT acts via Gs to stimulate transcytosis of occupied poly-Ig receptors and increase apical transport of vesicles bearing influenza hemagglutinin (Bomsel and Mostov, 1993; Pimplikar and Simons, 1993). Activation of Gs with CT also inhibits endosome fusion in J774 macrophages, a process thought to involve ARF (Colombo et al., 1994). The ARF-directed reagent BFA inhibits so-called constitutive secretion as well as insulin-triggered exocytosis of vesicles bearing the GLUT4 glucose transporter in rat adipocytes (Lachaal et al., 1994), Ca^{2+}-induced exocytosis of secretory granules in melanotrophs (Rupnik et al., 1995), cAMP-induced delivery of the cystic fibrosis transmembrane conductance regulator to the surface of human airway epithelial cells (Schwiebert et al., 1994), and recycling of transferrin receptors to the cell surface of K562 cells (Schonhorn and Wessling-Resnick, 1994). Further studies are necessary to determine whether ARF, through vesicle transport or other means, participates in the induction of I_{CRAC} via the FcεRI.

In summary, the potentiation of I_{CRAC} by CT does not result from direct modification of CRAC channel properties by Gs or CT. Nor is it an indirect result of membrane hyperpolarization or reduced rates of I_{CRAC} inactivation. The effect is restricted to antigen-induced I_{CRAC}, and the site of intervention apparently lies upstream of the CRAC channels themselves. It appears to be independent of phosphoinositide hydrolysis or the rate of Ca^{2+} release. Although other interpretations are tenable, the data suggest that FcεRI may act via ARF to enhance surface CRAC channel activity.

We are very grateful to Scott Schaus for writing the peak alignment macro for Ca^{2+} imaging data, and to Dr. George Ehring for critical comments on the manuscript.

This project was supported by National Institutes of Health grant GM48144.

Submitted: 26 April 1999
Revised: 2 December 1999
Accepted: 7 December 1999

References

Ali, H., K. Maeyama, R. Sagi-Eisenberg, and M.A. Beaven. 1994. Antigen and thapsigargin promote influx of Ca^{2+} in rat basophilic RBL-2H3 cells by ostensibly similar mechanisms that allow filling of inositol 1,4,5-trisphosphate-sensitive and mitochondrial Ca^{2+} stores. *Biochem. J.* 304:431–440.

Barsumian, E.L., C. Isersky, M.B. Petrino, and R.P. Siraganian. 1981. IgE-induced histamine release from rat basophilic leukemia cell lines: isolation of releasing and nonreleasing clones. *Eur. J. Immunol.* 11:317–323.

Beaven, M.A., J.P. Moore, G.A. Smith, T.R. Hesketh, and J.C. Metcalfe. 1984. The calcium signal and phosphatidylinositol breakdown in 2H3 cells. *J. Biol. Chem.* 259:7137–7142.

Berridge, M.J. 1995. Capacitative calcium entry. *Biochem. J.* 312:1–11.

Boman, A.L., and R.A. Kahn. 1995. Arf proteins: the membrane traffic police? *TIBS (Trends Biochem. Sci.).* 20:147–150.

Bomsel, M., and K.E. Mostov. 1993. Possible role of both the α and βg subunits of the heterotrimeric G protein, Gs, in transcytosis of the polymeric immunoglobulin receptor. *J. Biol. Chem.* 268:25824–25835.

Brown, H.A., S. Gutowski, C.R. Moomaw, C. Slaughter, and P.C. Sternweis. 1993. ADP-ribosylation factor, a small GTP-dependent regulatory protein,

stimulates phospholipase D activity. *Cell.* 75:1137–1144.

Buccione, R., S. Bannykh, I. Santone, M. Baldassarre, F. Facchiano, Y. Bozzi, G. Di Tullio, A. Mironov, A. Luini, and M.A. De Matteis. 1996. Regulation of constitutive exocytic transport by membrane receptors. A biochemical and morphometric study. *J. Biol. Chem.* 271:3523–3533.

Cockcroft, S., G.M.H. Thomas, A. Fensome, B. Geny, E. Cunningham, I. Gout, I. Hiles, N.F. Totty, O. Truong, and J.J. Hsuan. 1994. Phospholipase D: a downstream effector of ARF in granulocytes. *Science.* 263:523–526.

Colombo, M.I., L.S. Mayorga, I. Nishimoto, E.M. Ross, and P.D. Stahl. 1994. Gs regulation of endosome fusion suggests a role for signal transduction pathways in endocytosis. *J. Biol. Chem.* 269:14919–14923.

Colombo, M.I., J. Inglese, C. D'Souza-Schorey, W. Boron, and P.D. Stahl. 1995. Heterotrimeric G proteins interact with the small GTPase ARF. Possibilities for the regulation of vesicular traffic. *J. Biol. Chem.* 270:24564–24571.

De Matteis, M.A., G. Santini, R.A. Kahn, G. Di Tullio, and A. Luini. 1993. Receptor and protein kinase C-mediated regulation of ARF binding to the Golgi complex. *Nature.* 364:818–821.

Donaldson, J.G., and R.D. Klausner. 1994. ARF: a key regulatory switch in membrane traffic and organelle structure. *Curr. Opin. Cell Biol.* 6:527–532.

Fan, Y., and M.A. McCloskey. 1994. Dual pathways for GTP-dependent regulation of chemoattractant-activated K^+ conductance in murine J774 monocytes. *J. Biol. Chem.* 269:31533–31543.

Fanger, C.M., M. Hoth, G.R. Crabtree, and R.S. Lewis. 1995. Characterization of T cell mutants with defects in capacitative calcium entry: genetic evidence for the physiological roles of CRAC channels. *J. Cell Biol.* 131:655–667.

Fasolato, C., M. Hoth, and R. Penner. 1993. A GTP-dependent step in the activation mechanism of capacitative calcium influx. *J. Biol. Chem.* 268:20737–20740.

Fasolato, C., B. Innocenti, and T. Pozzan. 1994. Receptor-activated Ca^{2+} influx: how many mechanisms for how many channels? *TIPS (Trends Pharmacol. Sci.).* 15:77–83.

Hamilton, S.L., J. Codina, M.J. Hawkes, A. Yatani, T. Sawada, F.M. Strickland, S.C. Froehner, A.M. Spiegel, L. Toro, E. Stefani, et al. 1991. Evidence for direct interaction of Gsα with the Ca^{2+} channel of skeletal muscle. *J. Biol. Chem.* 266:19528–19535.

Helms, J.B. 1995. Role of heterotrimeric GTP binding proteins in vesicular protein transport: indications for both classical and alternative G protein cycles. *FEBS Lett.* 369:84–88.

Horn, R., and A. Marty. 1988. Muscarinic activation of ionic currents measured by a new whole-cell recording method. *J. Gen. Physiol.* 92:145–159.

Hosaka, M., K. Toda, H. Takatsu, S. Torii, K. Murakami, and K. Nakayama. 1996. Structure and intracellular localization of mouse ADP-ribosylation factors type 1 to type 6 (ARF1-ARF6). *J. Biochem.* 120:813–819.

Hoth, M. 1995. Calcium and barium permeation through calcium release-activated calcium (CRAC) channels. *Pflugers Arch.* 430:315–322.

Hoth, M., and R. Penner. 1992. Depletion of intracellular calcium stores activates a calcium current in mast cells. *Nature.* 355:353–356.

Hoth, M., and R. Penner. 1993. Calcium release-activated calcium current in rat mast cells. *J. Physiol.* 465:359–386.

Jouneaux, C., Y. Audigier, P. Goldsmith, F. Pecker, and S. Lotersztajn. 1993. G_s mediates hormonal inhibition of the calcium pump in liver plasma membranes. *J. Biol. Chem.* 268:2368–2372.

Kahn, R.A., and A.G. Gilman. 1986. The protein cofactor necessary for ADP-ribosylation of G_s by cholera toxin is itself a GTP binding protein. *J. Biol. Chem.* 261:7906–7911.

Klausner, R.D., J.G. Donaldson, and J. Lippincott-Schwartz. 1992. Brefeldin A: insights into the control of membrane traffic and organelle structure. *J. Cell Biol.* 116:1071–1080.

Lachaal, M., C. Moronski, H. Liu, and C.Y. Jung. 1994. Brefeldin A inhibits insulin-induced glucose transport stimulation and GLUT4 recruitment in rat adipocytes. *J. Biol. Chem.* 269:23689–23693.

Lewis, R.S., and M.D. Cahalan. 1989. Mitogen-induced oscillations of cytosolic Ca^{2+} and transmembrane Ca^{2+} current in human leukemic T cells. *Cell Regul.* 1:99–112.

Leyte, A., F.A. Barr, R.H. Kehlenbach, and W.B. Huttner. 1992. Multiple trimeric G-proteins on the trans-Golgi network exert stimulatory and inhibitory effects on secretory vesicle formation. *EMBO (Eur. Mol. Biol. Organ.) J.* 11:4795–4804.

Maguire, M.E., and J.J. Erdos. 1980. Inhibition of magnesium uptake by beta-adrenergic agonists and prostaglandin E_1 is not mediated by cyclic AMP. *J. Biol. Chem.* 255:1030–1035.

McCloskey, M.A. 1988. Cholera toxin potentiates IgE-coupled inositol phospholipid hydrolysis and mediator secretion by RBL-2H3 cells. *Proc. Natl. Acad. Sci. USA.* 85:7260–7264.

McCloskey, M.A. 1993. Immobilization of Fcε receptors by wheat germ agglutinin: receptor dynamics in IgE-mediated signal transduction. *J. Immunol.* 151:3237–3251.

McCloskey, M.A. 1999. New perspectives on Ca^{2+} influx in mast cells. *In* Signal Transduction in Mast Cells and Basophils. E. Razin and J. Rivera, editors. Springer-Verlag, New York. 227–246.

Millard, P.J., D. Gross, W.W. Webb, and C. Fewtrell. 1988. Imaging asynchronous changes in intracellular Ca^{2+} in individual stimulated tumor mast cells. *Proc. Natl. Acad. Sci. USA.* 85:1854–1858.

Morita, Y., and R.P. Siraganian. 1981. Inhibition of IgE-mediated histamine release from rat basophilic leukemia cells and rat mast cells by inhibitors of transmethylation. *J. Immunol.* 127:1339–1344.

Moss, J., and M. Vaughn. 1998. Molecules in the ARF orbit. *J. Biol. Chem.* 273: 21431–21434.

Murphy, P.M., and D. McDermott. 1992. The guanine nucleotide-binding protein Gs activates a novel calcium transporter in *Xenopus* oocytes. *J. Biol. Chem.* 267:883–888.

Narasimhan, V., D. Holowka, C. Fewtrell, and B. Baird. 1988. Cholera toxin increases the rate of antigen-stimulated calcium influx in rat basophilic leukemia cells. *J. Biol. Chem.* 263:19626–19632.

Penner, R., E. Neher, and F. Dreyer. 1986. Intracellularly injected tetanus toxin inhibits exocytosis in bovine adrenal chromaffin cells. *Nature.* 324:76–78.

Pimplikar, S.W., and K. Simons. 1993. Regulation of apical transport in epithelial cells by a Gs class of heterotrimeric G protein. *Nature.* 362:456–458.

Putney, J.W., Jr. 1990. Capacitative calcium entry revisited. *Cell Calcium.* 11: 611–624.

Putney, J.W., Jr. 1986. A model for receptor-regulated calcium entry. *Cell Calcium.* 7:1–12.

Randazzo, P.A., Y.C. Yang, C. Rulka, and R.A. Kahn. 1993. Activation of ADP-ribosylation factor by membranes. Evidence for a brefeldin A- and protease-sensitive activating factor on Golgi membranes. *J. Biol. Chem.* 268: 9555–9563.

Rudolph, A.K., P.D. Burrows, and M.R. Wabl. 1981. Thirteen hybridomas secreting hapten-specific immunoglobulin E from mice with Ig^a or Ig^b heavy chain haplotype. *Eur. J. Immunol.* 11:527–529.

Rupnik, M., G.J. Law, A.J. Northrop, W.T. Mason, and R. Zorec. 1995. Brefeldin A and a synthetic peptide to ADP-ribosylation factor (ARF) inhibit regulated exocytosis in melanotrophs. *Neuroreport.* 6:853–856.

Scamps, F., V. Rybin, M. Puceat, T. Vsevolod, and G. Vassort. 1992. A G_s protein couples P_2-purinergic stimulation to cardiac Ca channels without cyclic AMP production. *J. Gen. Physiol.* 100:675–701.

Schonhorn, J.E. and M. Wessling-Resnick. 1994. Brefeldin A down-regulates the transferrin receptor in K562 cells. *Mol. Cell. Biochem.* 135:159–169.

Schwiebert, E.M., F. Gesek, L. Ercolani, C. Wjasow, D.C. Gruenert, K. Karlson, and B.A. Stanton. 1994. Heterotrimeric G proteins, vesicle trafficking, and CFTR Cl^- channels. *Am. J. Physiol.* 267:C272–C281.

Thastrup, O., P.J. Cullen, B.K. Drobak, M.R. Hanley, and A.P. Dawson. 1990. Thapsigargin, a tumor promoter, discharges intracellular Ca^{2+} stores by specific inhibition of the endoplasmic reticulum Ca^{2+}-ATPase. *Proc. Natl. Acad. Sci. USA.* 87:2466–2470.

Yatani, A., J. Codina, Y. Imoto, J.P. Reeves, L. Birnbaumer, and A.M. Brown. 1987. A G protein directly regulates mammalian cardiac calcium channels. *Science.* 238:1288–1292.

Zhang, L., and M.A. McCloskey. 1995. Immunoglobulin E receptor-activated calcium conductance in rat mast cells. *J. Physiol.* 483.1:59–66.

Zweifach, A., and R.S. Lewis. 1993. Mitogen-regulated Ca^{2+} current of T lymphocytes is activated by depletion of intracellular Ca^{2+} stores. *Proc. Natl. Acad. Sci. USA.* 90:6295–6299.

Zweifach, A., and R.S. Lewis. 1995. Slow calcium-dependent inactivation of depletion-activated calcium current. *J. Biol. Chem.* 270:14445–14451.